PHYSICAL REVIEW A VOLUME 35, NUMBER 4 FEBRUARY 15, 1987

Properties of streamers and streamer channels in SF_6

R. Morrow
Division of Applied Physics, Commonwealth Scientific and Industrial Research Organization, P.O. Box 218, Lindfield, Sydney, Australia 2070
(Received 25 August 1986)

A theoretical examination is made of the mechanism of formation of cathode- and anode-directed streamers and the resultant ionized channel in SF_6, at 100 kPa, with a uniform applied field. The evolution of positive and negative ions, and electrons, is described by one-dimensional continuity equations, with the space-charged electric field determined by the method of disks. The main features of streamer formation may be understood by noting that any change in the electric field in SF_6 causes abrupt changes in the electron density N_e and current density J due to either strong net attachment or strong net ionization which balance at the critical field E^*. In the streamer head the net charge enhances the field ahead of the streamer and depresses the field behind, causing a rapid increase in N_e and J, followed by a rapid fall. The cathode-directed streamer propagates because photoionization releases electrons ahead of the streamer, while the anode-directed streamer can propagate, without photoionization, via electrons from the streamer head. The streamer channel is left with a uniform electric field $E_Q > E^*$ determined by a dynamic balance between conduction and displacement currents to maintain the total current.

I. INTRODUCTION

High-voltage technology has been greatly advanced by the use of compressed SF_6 gas as an insulating medium. For example, an SF_6-insulated substation occupies only 10% of the space occupied by a conventional atmospheric air substation and thus offers considerable economic and ecological advantages. There is therefore considerable interest in an improved understanding of electrical breakdown processes in SF_6, which show some unique features due to the highly electronegative character of the gas.

Recent studies[1-4] have shown that *streamers* form the first breakdown phenomena in SF_6. These streamers are ionizing waves moving in a very narrow channel towards either the cathode or the anode. The streamer leaves a thin ionized channel in the cold, neutral gas which subsequently develops into a highly conducting heated channel known as a *leader*. To understand breakdown and corona in SF_6 we need to explore the basic properties of anode- and cathode-directed streamers and of the ionized streamer channel. Knowledge of properties of the channel is important in predicting corona extensions and deposited charge in SF_6 point-plane discharges. These quantities underly the theory of leader onset.[1-3] For convenience we will refer to the ionized streamer channel as the "streamer trail."

This paper presents a theory of the structure of anode- and cathode-directed streamers and streamer channels in SF_6. We use one-dimensional continuity equations for electrons, positive ions, and negative ions (assuming equilibrium properties for the electrons), coupled to a three-dimensional approximation to Poisson's equation. This method was devised by Davies *et al.*[5] for streamers and has since been used by many other authors.[6-10] A full three-dimensional solution is a formidable task[11-14] and it is found that the quasi-one-dimensional approach adequately treats the general physics of the problem.[13]

The validity of the assumption that the electrons are in equilibrium with the electric field can be gauged by considering the work of Bayle and Cornebois,[15] who applied a similar method to streamers in nitrogen. By comparing solutions obtained with and without the equilibrium assumption, these authors found that the general streamer structure, particularly in the streamer channel, was not greatly influenced by the approximation. Kunhardt and Tzeng[11] have also solved Boltzmann's equation for streamer propagation in nitrogen, and concluded that "the fluid description is justified".

The basic equations used in the calculations are discussed in Sec. II, and the numerical results are presented in Sec. III under the following headings: A, avalanche phase; B, formation of the anode-directed streamer; C, formation of the cathode-directed streamer; D, secondary streamers; E, the streamer trail; and F, light output. These results are then analyzed in detail in Sec. IV and summarized in Sec. V.

II. THEORY

It is known from observation that streamers in SF_6 occupy a narrow cylindrical channel between the anode and the cathode.[1-4] We describe the axial development of this discharge by adopting one-dimensional continuity equations. We expect that ambipolar diffusion in the radial direction will act to confine the discharge, so that its radial expansion will be of secondary importance. Although one-dimensional continuity equations are used, we do take account of the finite radius of the discharge in solving Poisson's equation for the distribution of the axial electric field.

The one-dimensional continuity equations for electrons, positive ions, and negative ions, including ionization, pho-

toionization, attachment, recombination, and electron diffusion terms, are

$$\frac{\partial N_e}{\partial t}=S+N_e\alpha\,|\,W_e\,|\,-N_e\eta\,|\,W_e\,|\,-N_eN_p\beta - \frac{\partial(N_eW_e)}{\partial x}+\frac{\partial}{\partial x}D\frac{\partial N_e}{\partial x}\,, \tag{1}$$

$$\frac{\partial N_p}{\partial t}=S+N_e\alpha\,|\,W_e\,|\,-N_eN_p\beta-N_nN_p\beta-\frac{\partial(N_pW_p)}{\partial x}\,, \tag{2}$$

$$\frac{\partial N_n}{\partial t}=N_e\eta\,|\,W_e\,|\,-N_pN_n\beta-\frac{\partial(N_nW_n)}{\partial x}\,. \tag{3}$$

Here t is the time; x the distance from the cathode; N_e, N_p, and N_n the electron, positive-ion, and negative-ion densities, respectively; and W_e, W_p, and W_n are the electron, positive-ion, and negative-ion drift velocities, respectively. The symbols α, η, β, and D denote the ionization, attachment, recombination, and electron diffusion coefficients, respectively. The continuity equations are coupled to Poisson's equation via the charge density.

The term S is a source term due to photoionization and is given by

$$S(x)=\gamma_p\int_0^d \Omega(x-x')N_e(x')\alpha^*(x')\,|\,W_e(x')\,| \times\exp(-\mu\,|\,x-x'\,|\,)dx'\,, \tag{4}$$

where γ_p is the secondary ionization coefficient for photoionization, α^* the excitation coefficient for ionizing radiation, μ the coefficient of absorption, and Ω is the solid angle subtended at x' by the disk charge at x.

It is assumed that the transport properties of the gas (such as α and W_e) are determined by the reduced electric field E/N, where E is the local electric field and N is the neutral gas number density. A detailed survey of the electron and ion transport properties of SF_6 has been published elsewhere,[16] together with approximate analytical representations of the data which were used in this study.

The solution of Poisson's equation, calculation of the external circuit current, calculation of the light emitted, the treatment of the boundary conditions, and time step limitations are all as described in a previous study.[6] In the present study, secondary electron emission from the cathode is set to zero and the spatial mesh chosen to be uniform with 181 or 300 mesh points.

It can be shown that, given azimuthal symmetry and small radial terms, the continuity equations above, combined with a three-dimensional approximation to Poisson's equation, embody the Maxwell equation,[17]

$$\nabla\cdot\left[\mathbf{J}+\epsilon_0\frac{\partial\mathbf{E}}{\partial t}\right]=0\,, \tag{5}$$

where

$$\mathbf{J}=e(N_pW_p-N_nW_n-N_eW_e)\,. \tag{6}$$

The total current $\mathbf{J}'$,

$$\mathbf{J}'=\mathbf{J}+\epsilon_0\frac{\partial\mathbf{E}}{\partial t}\,, \tag{7}$$

will play an important role in the discussion of the streamer mechanism.

III. RESULTS

Results are presented for streamers propagating along a 100-μm-diam channel between parallel plate electrodes 0.5 cm apart, with an applied voltage of 46 kV, in SF_6 at 100 kPa. The calculation is initiated by the release of $\sim$400 seed electrons near the cathode at $t=0$. The computed current in the external circuit is shown in Fig. 1. The total formative time lag is about $\sim$10 ns, of which the first 7 ns is taken up with avalanche development, and the next 3 ns by streamers development. After the formative time lag, the gap is bridged by plasma and the circuit current rises sharply. We now present results for each separate aspect of the discharge development.

A. Avalanche phase

The electric field is 92 kV/cm initially compared with $E^*=89.6$ kV/cm, where E^* is the field at which $\alpha=\eta$. Thus the seed electrons multiply, forming an avalanche which has a peak density of 10^{12} cm^{-3} centered at $x=0.17$ cm after 7.2 ns. The corresponding peak positive- and negative-ion densities are 7×10^{12} and 6×10^{12} cm^{-3}, respectively, as shown in Figs. 2 and 3. The circuit current is very small at this time (see Fig. 1); however, after 7 ns have elapsed, space-charge effects set in (Fig. 4), leading to streamer development since the net ionization increases sharply with electric field.

B. Formation of the anode-directed streamer

The peak in electron density moves rapidly from $x=0.17$ cm at time $t=7.2$ ns to $x=0.28$ cm at time $t=9.24$ ns (see Fig. 5) due to space-charge effects associated with a negative peak in the net charge (e.g., $x=0.28$ cm and $t=9.24$ ns in Fig. 6). This peak in negative

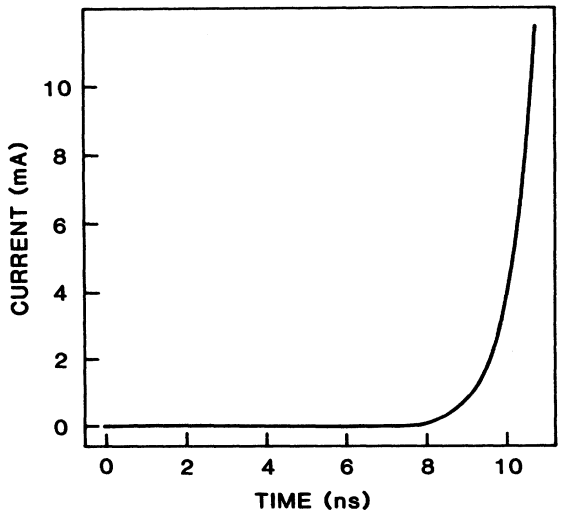

FIG. 1. Computed current in the external circuit vs time.

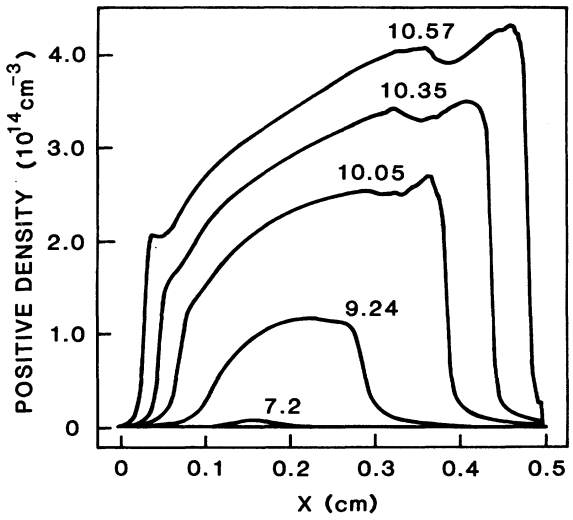

FIG. 2. Positive-ion density vs position at the times shown (ns) after the release of the initial seed electrons. The cathode is at $x=0$ cm and the anode at $x=0.5$ cm.

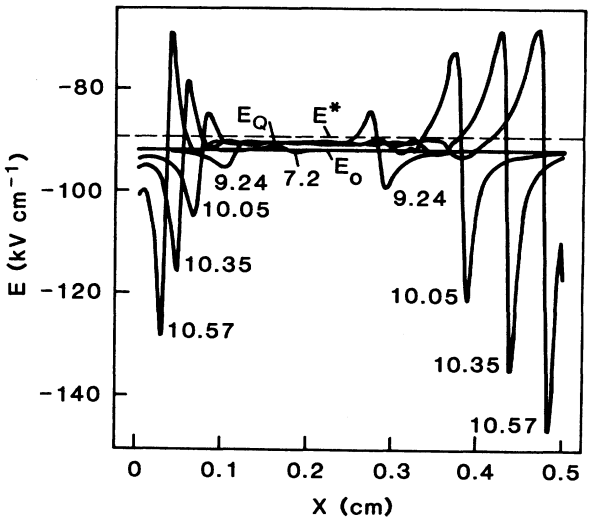

FIG. 4. Electric field vs position at various times (ns). E_0 is the initial field, E^* is the critical field at which $\alpha=\eta$, and E_Q is the equilibrium field in the streamer trail.

charge, due to electrons [see Figs. 2, 3, 5, and 7(b)], acts like a point charge with field enhancement on the anode side of the charge center, and field depression below E^* on the cathode side (Fig. 4). The field enhancement promotes rapid ionization followed by rapid attachment as the streamer passes. The electron cloud and corresponding field distortion grow rapidly, as shown in Figs. 4, 5, and 6, and the streamer head moves with a uniform velocity of 1.75×10^8 cm s^{-1} (Fig. 8), reaching the anode in 1.5 ns. The negative charge in the streamer head increases steadily from 2×10^7 to 4×10^7 electrons, as shown in Fig. 9, and the current rises rapidly, as shown in Fig. 1.

C. Formation of the cathode-directed streamer

The cathode-directed streamer is associated with a positive peak in the net charge (e.g., $x=0.1$ cm, $t=9.24$ ns, in Fig. 6), which causes a field distortion in the opposite sense to that caused by the negative charge of the anode-directed streamer described above (see Fig. 4). The field is enhanced in the direction of propagation, on the cathode side of the positive charge center, and depressed on the anode side.

Note that there is a peak in the electron density which follows the peak in the net charge, as shown in Figs. 5 and 7(a). The streamer velocity is 8.25×10^7 cm s^{-1} (Fig. 8), which is 50% less than that for the anode-directed strea-

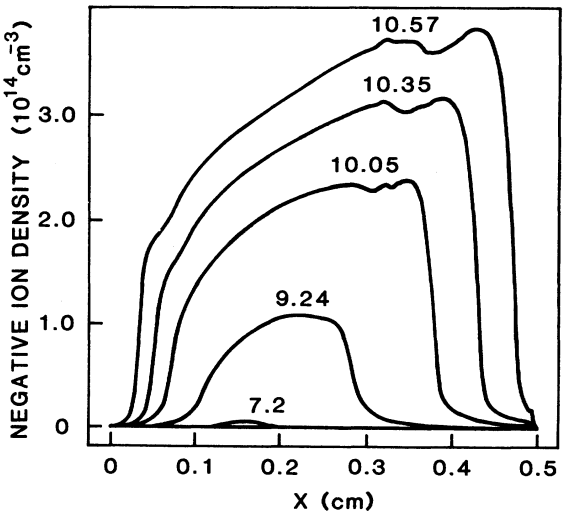

FIG. 3. Negative-ion density vs position at various times (ns).

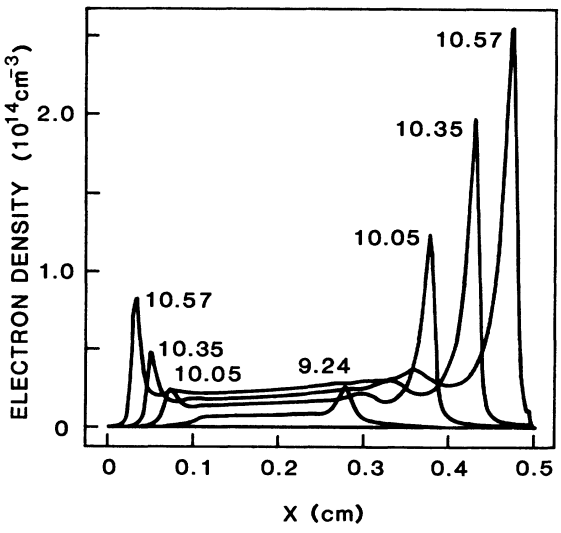

FIG. 5. Electron density vs position at various times (ns).

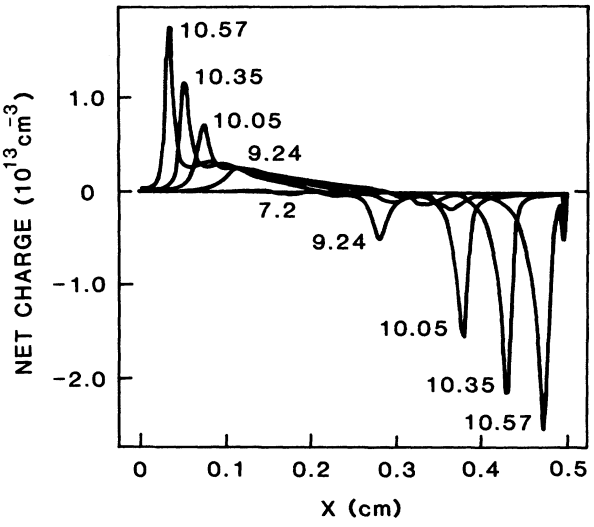

FIG. 6. Net charge density vs position at various times (ns).

mer; the net charge in the streamer head is also less (Fig. 9).

D. Secondary streamers

Secondary streamers are characterized by the enhancement of the field behind the main ionizing wave of both streamers, such as at $x=0.38$ cm and $t=10.57$ ns for the anode-directed secondary streamer, and at $x=0.07$ cm and at $t=10.57$ ns for the cathode-directed secondary streamer (Fig. 4). The passage of the anode-directed secondary streamer causes the second maxima in the electron, positive-ion, and negative-ion densities at $x=0.36$ cm, $t=10.57$ ns in Figs. 5, 2, and 3, respectively. Unfortunately, the predicted light output from the secondary streamer (shown in Fig. 10) is only slightly greater than that expected from the streamer trail, making the experimental detection of such effects difficult.

E. The streamer trail

The electric field in the streamer trail adjusts to a uniform, relatively fixed value E_Q, just larger than E^*, after the passage of either streamer head. The electron density and light output from the trail are relatively uniform and increase with time, as shown in Figs. 5 and 10. The positive- and negative-ion distributions are similar (Figs. 2 and 3) and combine with the electron distribution to give a net charge density grading smoothly from positive to negative (Fig. 6); this gradation maintains the uniform field in the narrow channel, as discussed by Morrow.[18]

F. Light output

The light output (shown in Fig. 10) shows sharply defined points of light associated with the streamer heads, moving towards each electrode while growing in amplitude. Between the streamers a relatively uniform low lev-

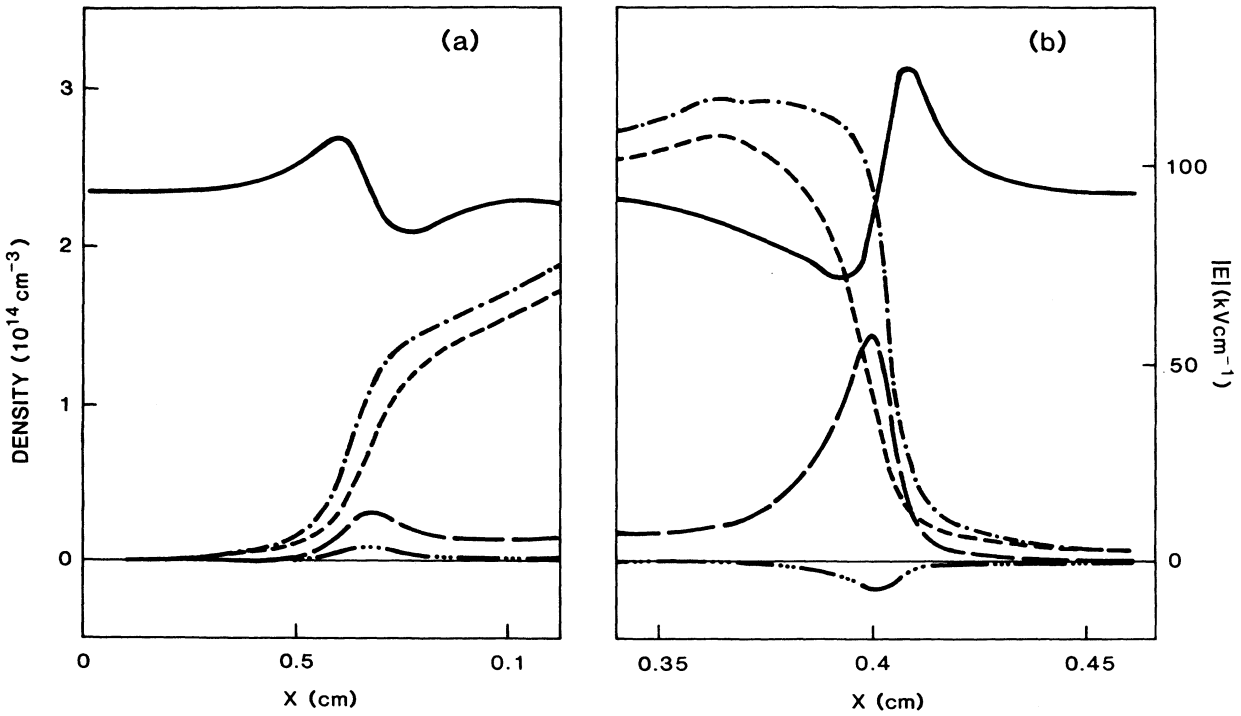

FIG. 7. Structure of (a) the cathode-directed streamer, (b) the anode-directed streamer at $t=10.16$ ns. Electric field amplitude, ——; positive-ion density, —·—·—·; negative-ion density, — — —; electron density, ———; net charge density, —···—···.

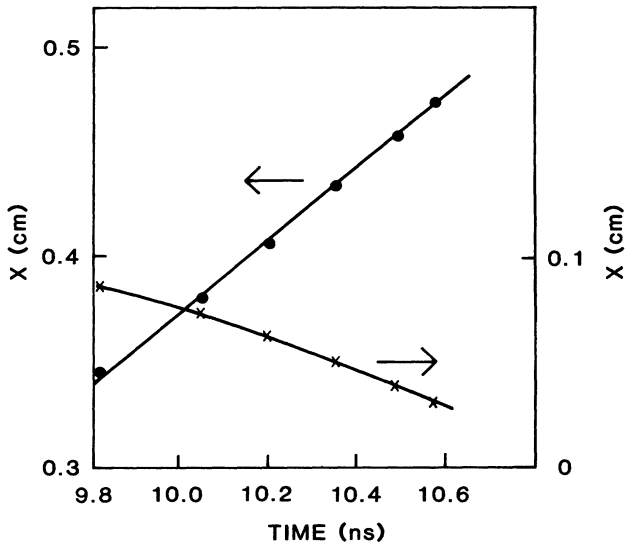

FIG. 8. Position of the streamer maximum charge density vs time. ●, anode-directed streamer; ×, cathode-directed streamer.

el of light output is predicted with only slight inflections where the secondary streamers occur.

IV. DISCUSSION

In this section we discuss the bearing of our results on the explanation of the origins of the various features found in SF_6 streamer propagation. Seven separate aspects will be considered.

A. Avalanche phase

The avalanche-to-streamer transition is predicted by Pedersen's criterion[19]

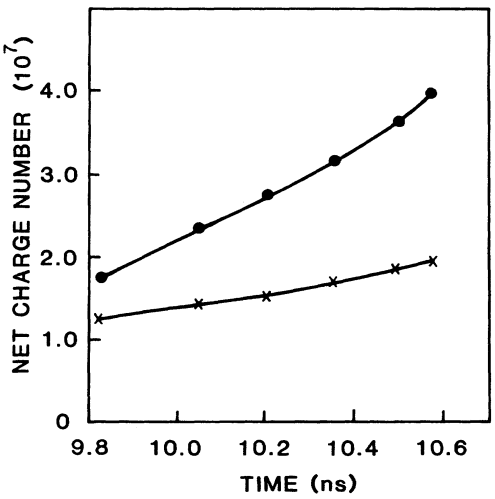

FIG. 9. Net charge density in the streamer head vs time. ●, anode-directed streamer; ×, cathode directed streamer.

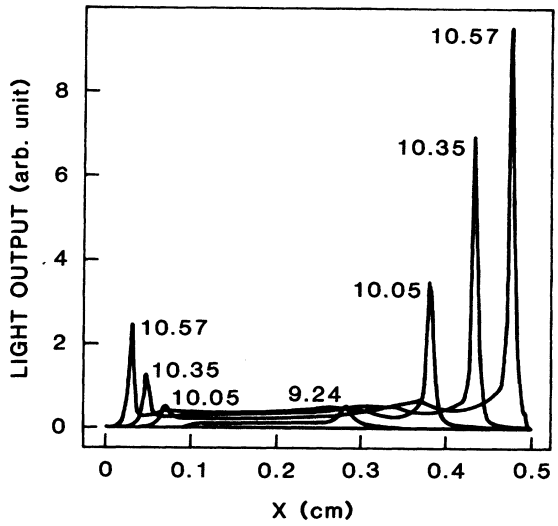

FIG. 10. Light output (arbitrary units) vs position for various times (ns).

$$\int_0^{\lambda} (\alpha - \eta) dx = 18 \tag{8}$$

to occur after the avalanche has traveled a distance $\lambda \geq 0.22$ cm, which agrees well with the results in Fig. 4. The criterion predicts the presence of 6×10^7 electrons in the avalanche at that time; this is somewhat larger than the value shown in Fig. 9 for the number of electrons in the streamer head. Note that the positive- and negative-ion densities in SF_6 avalanches are almost an order of magnitude greater than the electron density.

B. Static interpretation of streamer propagation

It is clear from Fig. 7 that attachment dominates all aspects of streamer formation in SF_6; for example, the negative-ion density is always larger than the electron density except for a small region of the anode-directed streamer head [Fig. 7(b)]. Photoionization in front of both streamers liberates electrons, which then ionize, since $E > E^*$, but which also attach to produce negative ions. The negative-ion density that develops is just less than the positive-ion density, while the electron density is an order of magnitude less (Fig. 7). In the streamer trail ionization continues at a rate sufficient to maintain the conductivity against electron losses due to attachment, which causes a steadily rising negative-ion density.

In the head of both streamers the increase in ionization activity (shown by the rise in N_p in Fig. 7) starts with the rise of the electric field and continues as the field falls due to the increased electron density in this region. The negative-ion density follows this rise in positive-ion density through the ionizing wave front, since attachment is still very strong, even though $\alpha > \eta$, and newly released electrons are rapidly attached.

The role of electron drift at any instant, in either wave front, is made clear by considering the "new" plasma, created at that instant, which will have no space-charge effect until charge separation occurs due to electron drift.

In the case of the cathode-directed streamer the electrons will move towards the anode, revealing new positive charge and neutralizing the space-charge effect of some of the "old" positive charge; thus the center of net positive charge [Figs. 6 and 7(a)] and the corresponding field distortion [Figs. 4 and 7(a)] move towards the cathode. In the case of the anode-directed streamer, the electrons from the "new" plasma move towards the anode, revealing their own negative charge, while the space-charge effect of the advancing electron-density maximum is neutralized by the "new" positive charge; thus the center of net negative charge [Figs. 6 and 7(b)] and corresponding field distortion [Figs. 4 and 7(b)] move towards the anode. Behind each kind of streamer the electric field is depressed below E^* and electrons attach rapidly, giving a sharp electron-density fall after the peak.

Thus α determines the rate of creation of "new" plasma, drift determines the rate of charge separation, and η plays a dominant role in attaching the electrons and making them relatively immobile, thereby limiting the number of electrons which can drift to move the charge centers.

Photoionization provides electrons ahead of the advancing field maxima for both streamers [Figs. 7(a) and 7(b)]. It is essential for the propagation of the cathode-directed streamer which is very sensitive to changes in this process, while the anode-directed streamer is less sensitive. When photoionization is set to zero, cathode-directed streamers are not formed while the velocity of anode-directed streamers is 50% less than that shown in Fig. 8.

C. Dynamic interpretation of streamer propagation

The interaction between the conduction and displacement currents in the streamer can be understood by rearranging Eq. (7) (noting that both $\mathbf{J}$ and $\mathbf{J}'$ are negative) to give

$$\frac{\partial \mathbf{E}}{\partial t}=\frac{1}{\epsilon_0}(\,|\mathbf{J}|-|\mathbf{J}'|\,)\,. \tag{9}$$

Thus, when the current J develops in the streamer channel, $\partial E/\partial t$ must be negative between the streamer head and the electrodes, where the conduction current is zero. Near the electrodes, this displacement current density is distributed over a large area and $|\partial E/\partial t|$ is therefore small, while near the streamer tip $|\partial E/\partial t|$ reaches a maximum. As the electric field reaches a maximum, the electron density rises rapidly (Fig. 7), and so does $|J|$, which causes $\partial E/\partial t$ to become positive via Eq. (9). Thus $|E|$ falls rapidly, eventually below $|E^*|$, and electrons attach, reducing J. If J falls too far, the $\partial E/\partial t$ term again becomes negative and secondary streamers may result as an overshoot effect.

Thus once the initial transients in the electric field have passed, any significant deviation in E away from E^* leads to rapid changes in N_e and concomitant changes in $\partial E/\partial t$, restoring the electric field back to a value close to E^*. (I am indebted to Dr. J. J. Lowke for first pointing out the importance of E^* in SF_6.) We can quantify this effect by evaluating the characteristic time τ for changes in the electron density, using the formula

$$\tau=1/[(\alpha-\eta)\,|\,W_e\,|\,]\,. \tag{10}$$

For a value of $E=0.97E^*$, $\tau\approx 5\times 10^{-10}$ s and N_e and J fall rapidly, while for $E=1.03E^*$, $\tau\approx 6\times 10^{-10}$ s and N_e and J increase very rapidly.

Alternatively we can rewrite Eq. (8) for the case $E<E^*$ in the form

$$\int_0^{\lambda}(\eta-\alpha)dx=\ln(10)=2.3 \tag{11}$$

and find the value of E for which N_e decreases by an order of magnitude in a distance λ. For $\lambda=0.1$ cm the value of E which satisfies Eq. (11) is only 0.7% less than E^*. Thus the field in the streamer trail must be confined between the values defined by Eqs. (8) and (11). The electric field adjusts to a value E_Q which supports the conduction current and its growth.

We can derive an expression for the current in the streamer channel, I, as a function of E if we assume that $\partial E/\partial t=0$ and that the current density J is due to electrons and is uniform over the channel area A:

$$I(t)=-Ae\mu_e\,|\,E\,|\,N_e(0)\exp[(\alpha-\eta)\mu_e\,|\,E\,|\,t]\,, \tag{12}$$

where $W_e=-\mu_e E$, μ_e is the electron mobility, and $N_e(0)$ is the electron density at the time $t=0$ when the streamer channel is established. Thus if $I(t)$ increases in time and E changes slowly, we require $\alpha>\eta$ and $E=E_Q>E^*$.

The properties of the streamer trail have also been considered by Andersson[20] and Bastien and Marode,[21] who found that the electric field in the trail was higher for attaching gases than for nonattaching gas. Andersson considered the minimum applied field for streamer propagation, the streamer "guiding field," and showed both theoretically and experimentally that this field is higher in gases with larger attachment coefficients due to the necessity of maintaining the channel conductivity.

D. Comparison with other gases

We can predict the likely behavior of the electric field in the streamer trail of various gases at atmospheric pressure by evaluating the following critical values of the electric field:

(1) E_1 satisfying Eq. (8) for $\lambda=0.22$ cm,
(2) E^* satisfying $\alpha(E^*)=\eta(E^*)$, and
(3) E_2 satisfying Eq. (11) for $\lambda=0.1$ cm.

The resulting values are shown in Table I for SF_6, O_2, air, and N_2.

Thus, as discussed above, the field in the streamer trail in SF_6 is confined to a vary narrow range of E to maintain conductivity, while in O_2 this range could be much wider. Thus O_2 forms an interesting intermediate case between SF_6 and both air and nitrogen, where there is no lower value of the electric field at which conduction ceases. In agreement with this, Davies *et al.*[5] found theoretically that in nitrogen the electric field in the streamer trail was not bounded, but was able to vary while maintaining the channel conduction via both conduction and displacement currents. We expect the same behavior for air and, in fact, experimental results confirming these trends have recently been obtained by Gallimberti *et al.*[22]

TABLE I. Comparison of the critical electric fields for various gases (kV cm^{-1}).

Gas	SF_6	O_2	Air	N_2
E_1	92	43	44.8	49.8
E^*	89.6	33.4	$\approx$23.5	
E_2	89	29.5		

E. Corona extensions and the guiding field

The results presented in this paper have immediate consequences for discharges in nonuniform electric fields in SF_6 since a streamer emanating from a point electrode must leave a streamer trail behind it with an electric field $E_Q > E^*$. The extent to which a streamer may propagate out into the gap leaving such a trail will be limited via the equation

$$V_A = \int_0^d E \cdot ds \ , \tag{13}$$

where V_A is the applied voltage and d the electrode spacing. If the electric field in the streamer trail is $E \simeq E^*$, then the maximum corona extension l_c is given by

$$V_A = E^* l_c \ . \tag{14}$$

This result has been used to predict corona extensions and charges in SF_6.[1-3]

The result also has consequences for the concept of the streamer guiding field in SF_6 proposed by Chalmers *et al.*[4] From the discussion above it is evident that streamer propagation cannot be sustained in SF_6 with an electric field less than E^*, otherwise $l_c < d$ and the streamers cannot bridge the gap. Much experimental evidence has now been accumulated to support this view.[1-3,22]

F. Light output and the external circuit current

Light absorption in SF_6 is so great that there are very few observations of the prebreakdown light output. However, recent observations by Gallimberti *et al.*[22] in a point-plane gap show a pulse of light moving at almost constant velocity, with decreasing amplitude during the advance; here too we find constant velocity, although the predicted streamer amplitude increases with time (Fig. 8). In other gases it is found that streamer luminosity increases as the streamers cross a uniform field gap,[23] and in air[24] and nitrogen[25] the streamer front is seen as a moving point of light.

The predicted external circuit current (Fig. 1) is similar to the experimental observations of Raether[26] in air where he finds a very small current for the prestreamer phase and then a rapid rise in the circuit current corresponding to the development of streamers. The extremely rapid current rise time is in qualitative agreement with the observations of Biesselmann *et al.*[27]

G. Comparison with three-dimensional results

With the present approach the channel diameter must be specified beforehand. It is of interest to compare the value used in this study (100 μm) with those found in theoretical studies where the channel diameter is determined as part of the solution to the problem. Bortnik *et al.*[12] found a value of 200 μm, while Kunhardt and Tzeng[11] found a value of 50 μm for the cathode-directed streamer and 100 μm for the anode-directed streamer. Dhali and Williams[13] found that the predicted streamer diameter could vary depending on the starting conditions and pointed out that this may account for some of the variability in streamer properties. From experimental and theoretical studies of leaders in SF_6, Niemeyer[28] estimated the width of the streamer channel to be $\sim$70–100 μm at 100 kPa.

Dhali and Williams[13] and Kunhardt and Tzeng[12] have found the anode-directed streamer to propagate faster than the cathode-directed streamer. Kunhardt and Tzeng found the ratio to be two, as we have predicted (Sec. III), and the critical number of electrons in the avalanche to be 10^8.

Bortnik *et al.*[12] and Kunhardt and Tzeng[11] have predicted several maxima and minima in the electric field. Kunhardt has described "parent" and "secondary" avalanches, which we believe correspond to our secondary streamer phenomena.

Kunhardt and Tzeng[11] have also evaluated the effect of neglecting photoionization and found that the cathode-directed streamer does not propagate and that the anode-directed streamer propagates more slowly. Our results are consistent with their predictions.

V. CONCLUSIONS

The mechanism of streamer development in SF_6 has been clearly outlined in this paper. The results obtained for streamer onset are shown to agree very well with criteria developed by Pedersen and others. The complex interrelationships between ionization, electron drift, attachment, and space-charge effects in the streamer front have been elucidated, as well as the factors leading to the development of secondary streamers. The prediction of discrete points of light moving at relatively constant velocity (even though the intensity varies considerably) agrees with measurements in SF_6 and other gases. The light output from the secondary streamers is expected to be too weak to detect. The predicted form of the circuit current agrees with previous experimental studies in air and SF_6.

A unifying concept has been proposed by Fernsler,[29] namely, that "a streamer propagates by transforming conduction current in its body into displacement current at its tip." Thus we are alerted to concentrate on conductivity and current densities rather than N_e and E alone. The abrupt change in properties at a high value of electric field, E^*, leads to a complex interrelation between conduction and displacement currents which produces a propagating transient in the electric field associated with the streamer, much like a soliton wave. Associated with this transient behavior there may be one or more secondary peaks in the electric field which give rise to what we have termed "secondary streamers." The numerical results and discussion show that the field in the streamer trail must remain at a uniform value, E_Q, high enough to

maintain the conductivity. This feature, although it appears static, is in fact a dynamic equilibrium between the conduction and displacement currents. It may be inferred that the condition $E_Q > E^*$ is also required for streamer formation in nonuniform fields, and as a result the distance a streamer can propagate in a point-plane gap in SF_6 can be estimated; also, as a result, the "guiding field" for streamers in SF_6 is limited by $E_g \geq E^*$.

ACKNOWLEDGMENTS

I am indebted to Professor Owen Farish for introducing me to the study of SF_6 streamers and for guiding me in the early part of this work. I acknowledge stimulating discussions with Professor I. Gallimberti, Dr. A. Pedersen, and Dr. J. J. Lowke, and the continued guidance and support of Dr. L. E. Cram. I would also like to acknowledge discussions with Dr. F. Pinnekamp, Dr. L. Niemeyer, and Dr. N. J. Wiegart, and the Brown Boveri Company and thank that company for their interest and hospitality. I thank Dr. R. Loughhead for helpful discussions and advice and thank both him and Ms. V. M. Bowers for their help in writing the manuscript. Finally, I acknowledge the generous support of the Canadian Electrical Association for the study on SF_6 breakdown; this work was part of that study.

[1]The Canadian Electrical Association (CEA) Report No. 153T310, 1985 (unpublished).
[2]N. J. Wiegart, in *Eighth International Conference on Gas Discharges and their Applications, Oxford, 1985,* edited by N. L. Allen (Institute of Electrical Engineers, London, 1985), pp. 227–230.
[3]I. Gallimberti and N. J. Wiegart, in Ref. 2, pp. 219–222.
[4]I. D. Chalmers, O. Farish, and S. J. MacGregor, in *Proceedings of the Fourth International Symposium on Gaseous Dielectrics, Knoxville, U. S. A.,* edited by L. G. Christophorou and M. O. Pace (Pergamon, New York, 1984), pp. 344–353.
[5]A. J. Davies, C. S. Davies, and C. J. Evans, Proc. Inst. Electr. Eng. **118**, 816 (1971).
[6]R. Morrow, Phys. Rev. A **32**, 1799 (1985).
[7]L. E. Kline, J. Appl. Phys. **45**, 2046 (1974); **46**, 1994 (1975).
[8]K. Yoshida and H. Tagashira, J. Phys. D **9**, 485; **9**, 491 (1976).
[9]P. Bayle and M. Bayle, Z. Phys. **266**, 275 (1974).
[10]R. Morrow, Phys. Rev. A **32**, 3821 (1985).
[11]E. E. Kunhardt and Y. Tzeng, in Ref. 4, p. 146.
[12]I. M. Bortnik, I. I. Kochetov, and K. N. Ul'yanov, Teplofiz. Vys. Temp. **20**, 193 (1982) [High Temp. (USSR) **20**, 165 (1982)].
[13]S. K. Dhali and P. F. Williams, Phys. Rev. A **31**, 1219 (1985).
[14]A. J. Davies, C. J. Evans, P. Townsend, and P. M. Woodison, Proc. Inst. Electr. Eng. **124**, 179 (1977).
[15]P. Bayle and B. Cornebois, Phys. Rev. A **31**, 1046 (1985).
[16]R. Morrow, IEEE Trans. Plasma Sci. **PS-14**, 234 (1986).
[17]B. I. Bleaney and B. Bleaney, *Electricity and Magnetism* (Clarendon, Oxford, 1959).
[18]R. Morrow, J. Comput. Phys. **46**, 454 (1982).
[19]A. Pedersen, IEEE Trans. Power Appar. Syst. **PAS-89**, 2043 (1970).
[20]N. E. Andersson, Ark. Fys. **13**, 399 (1958); **13**, 441 (1958).
[21]F. Bastien and E. Marode, J. Phys. D **18**, 377 (1985).
[22]I. Gallimberti, G. Marchesi, and R. Turri, in Ref. 2, pp. 167–170.
[23]L. B. Loeb, Science **148**, 1417 (1965).
[24]G. G. Hudson and L. B. Loeb, Phys. Rev. **123**, 29 (1961).
[25]K. H. Wagner, Z. Phys. **189**, 465 (1966).
[26]H. Raether, *Electron Avalanches and Breakdown in Gases* (Butterworths, London, 1964).
[27]M. Biesselmann, I. Kusuma, W. Pfeiffer, and J. Wolf, in Ref. 2, p. 278.
[28]L. Niemeyer (private communication).
[29]R. F. Fernsler, Phys. Fluids **27**, 1005 (1984).